

INTERNATIONAL SOCIETY FOR SOIL MECHANICS AND GEOTECHNICAL ENGINEERING



This paper was downloaded from the Online Library of the International Society for Soil Mechanics and Geotechnical Engineering (ISSMGE). The library is available here:

<https://www.issmge.org/publications/online-library>

This is an open-access database that archives thousands of papers published under the Auspices of the ISSMGE and maintained by the Innovation and Development Committee of ISSMGE.

A method for estimating squeezing earth pressures acting on a deep tunnel

R. Nakano, H. Shimizu & S. Nishimura
 Faculty of Agriculture, Gifu University, Japan

SYNOPSIS: Swelling pressure often experienced in deep tunnels through relatively soft mudstone or its fault clay has long been explained to be caused by swelling of clay minerals (such as Montmorillonite) due to their sucking up of water. This is the reason why the swelling test of clay is specified by "Standard design specification for tunnels" published by JSCE (Japanese Society of Civil Engineers). Both case history and studies based on Critical State Soil Mechanics' concept have been undertaken to investigate if this explanation is really correct. Incorporating shear strength parameters in terms of total and effective stresses, for short-term and long-term problems respectively, into modified Kastner's classical approach, clear evidence has been given that the predominant cause of large mountain pressure encountered in the so-called swelling tunnels is the plastic flow of the broken material and not the swelling of it.

1 INTRODUCTION

In Japan, argillaceous rocks such as mudstone or shale, especially those of Neogene deposit, often cause troubles in geotechnical engineering, among which the so-called swelling pressure on tunnel support is the typical one. Referring to the swelling rock in tunneling, it is written by Terzaghi (1964). "The pressure on the support in tunnels through swelling rock depends primarily on the swelling capacity of the rock which is analogous to the swelling capacity of clays".

The aim of this paper is to elucidate the real cause of swelling tunnel pressure denying Terzaghi's explanation quoted above and to reconfirm quantitatively the explanation presented by Nakano (1979).

2 CASE HISTORY OF NABETACHIYAMA TUNNEL

Nabetachiyama Tunnel, 9,117m long single truck railway tunnel, is located in the southern part of Niigata Prefecture, and occupies the middle part of the route of the Hokuetsu North Line, having been constructed under the supervision of JRCP (The Japan Railway Construction Public Corporation). This tunnel is divided into three work sections (west, middle & east), among which east section (29k573m50~31k324m) and west section (34k711m~38k690m) had been completed in Aug. 1978 and in March 1982 respectively. However, as the middle section (31k324m~34k711m) suffered from a very heavy earth pressure, the excavation was discontinued in March 1982, leaving the unexcavated length 645m between 32k404m~33k049m, the excavation of which was resumed in Aug. 1985 and a pilot central drift was driven through in Oct. 1992.

Fig.1(a) gives the longitudinal profile of the mountain along the Nabetachiyama Tunnel and the nature of folding. The middle work section of this mountain mainly composed of Shiya formation are severely folded and faulted into clay by overfolds which contain inflammable gas (mostly methane).

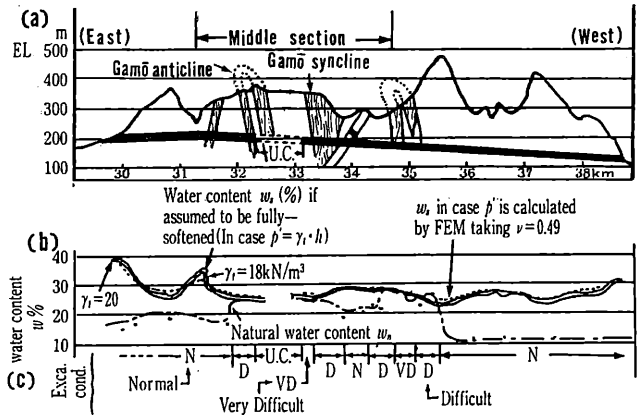


Fig.1 Profile of Nabetachiyama Tunnel
 (a) Profile of Nabetachiyama Mountain
 (b) Distribution of natural water content w_n and water content w_s to be attained if fully-softened to critical state
 (c) Excavation condition (U.C.: Under Construction)

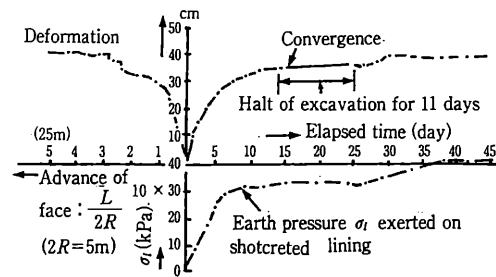


Fig.2 Increase in earth pressure and convergence in relation to the advance of tunnel face and elapsed time

According to the construction records by Ohtsuka(1980), the excavation through these zones was very difficult due to very heavy pressure although NATM with sliding supports (MU-29), rockbolts and shotcrete($t=12\text{cm}$) was employed. The natural water content distribution and excavation condition are also given in Fig.1(b), (c).

Between 33k140m~33k204m, severely disturbed zone by Gamo-folding, an advancing center circular drift with a diameter of $2R_1=5\text{m}$ was driven to measure earth pressure and convergence. A typical example of these observed data is given in Fig.2. The earth pressure distribution around the tunnel when the pressure had reached an equilibrium was also reported by Kojima(1990), very hydrostatic distribution being confirmed.

3. SOIL MECHANICAL PROPERTIES OF MUDSTONE

Physical properties of the faulted mudstone from the middle work section are $w_L = 155\%$, $w_p = 27\%$, $I_p = 128\%$, $\rho_s = 2.75$, $CF = 70\%$. Blocks of clay were also sampled and their undisturbed strengths were obtained by unconsolidated undrained(UU) triaxial test. To measure the mechanical properties of the fault clay at fully softened state, triaxial consolidated drained(CD) and consolidated undrained(CU) tests were also carried out on reconstituted 35mm dia. specimens normally consolidated from slurry, using top and bottom drainage only to minimize the non-uniformity of water content (Atkinson(1985)).

Fig.3 shows the relationships between compressive strength q , Young's modulus E_{cu} and water content and Fig.4 shows the relationship between water content and average effective confining stress $p' = (\sigma_1' + 2\sigma_3')_{max}/3$ at the end of each test.

The water contents in these Figures are w_s at fully softened state and the strengths are also those of the corresponding state, ϕ_s and c_s by CD test being respectively 17° and 0 kPa .

Assuming the coefficient of lateral earth pressure $K = 1$, which is generally accepted appropriate for overconsolidated clay or mudstone in depth, the effective average confining stress p' at various locations along the tunnel was calculated taking $p' = \gamma_t \cdot h$ (h : overburden depth). The fully-softened state water content corresponding to this p' was calculated by the formulae given in Fig.4, and is plotted along the tunnel as shown in Fig.1(b) showing the natural water content w_n in the very difficult section was nearly the same with the value calculated

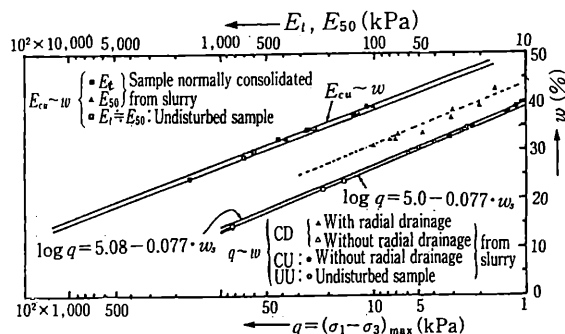


Fig.3 Relationships between compressive strength q , Young's modulus E_{cu} and water content w

above, i.e., the mudstone in this section is at fully-softened state.

4. SIMPLE ANALYTICAL APPROACH

In order to conduct a simple analysis with simplified boundary conditions to obtain an estimate of the solution without losing physical insight into the problem, Kastner's approach (Kastner(1962)) is adopted with some modifications based on modern soil mechanics.

As the heavy pressure exerted on tunnel support is hydrostatic and the stress-strain relationship of the faulted mudstone at fully softened state is nearly of perfect plasticity showing no strain softening, the assumptions to derive Kastner's formulae are the same with the actual conditions of the present case. However, since no effective stress concept had been taken into account in deriving the original formulae, we must be careful in choosing strength parameters, i.e. distinction should be made between short-term and long-term after construction.

4.1 Stress and deformation around a circular tunnel

By the mathematical manipulation of Kastner's original formulae and on the assumption that the plastic zone is squeezed into the tunnel space by the deformation U_s of the elastic zone, the stresses (σ_r, σ_θ), converging deformation U_s of tunnel wall and average confining stress p can be obtained by the formulae shown in Table 1 (For the meaning of symbols ref. Fig.5)

In case of long-term, the effective strength parameters $c = c_u = 0$ ($q_u = 0$), $\phi_u = 17^\circ$ should be substituted into the equations (1), (2) and p thus calculated is the effective stress p' . In case of short-term, as strength parameters $c = c_u = q_u/2$, $\phi = \phi_u = 0^\circ$, taking the limit ($\zeta \rightarrow 1$) of equations (1) (2), equations (6) and (7) are obtained and p calculated by equation (10) is of total stress. It should be noted here, however, that the average effective confining stress p' at short-term is kept constant at a value before a tunnel is excavated because negative pore pressure $u < 0$ develops, for this reason $\phi_u = 0$ method being justified (Skempton(1963)).

5. APPLICATION TO NABETACHIYAMA TUNNEL

5.1 Relation between earth pressure and convergence

Between 33k140m~33k204m under an approximate

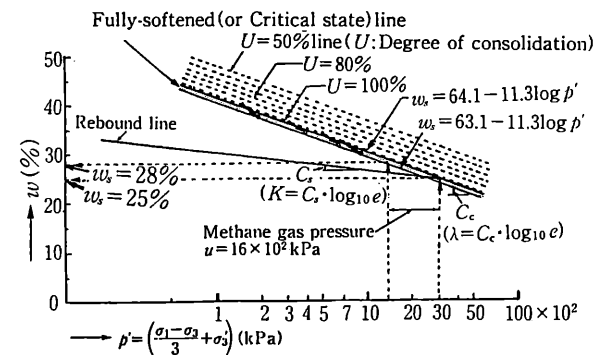


Fig.4 Relationship between average effective confining stress p' and water content w

Table 1. Formulae for stresses and deformations in plastic zone around a tunnel

Long-term after excavation (effective stress)		Short-term after excavation (total stress)	
$\sigma'_r = \frac{q_u}{\zeta - 1} \left[\left(\frac{r}{R_1} \right)^{\zeta - 1} - 1 \right] + \sigma_i \left(\frac{r}{R_1} \right)^{\zeta - 1}$... (1)	$\sigma_r = \sigma_i + q_u \ln \frac{r}{R_1}$... (6)
$\sigma'_\theta = \zeta \cdot \sigma'_r + q_u$... (2)	$\sigma_\theta = \sigma_r + q_u$... (7)
$\frac{R_a}{R_1} = \left\{ \frac{2}{1 + \zeta} \cdot \frac{\zeta - 1 + F_c}{\beta(\zeta - 1) + F_c} \right\}^{\frac{1}{\zeta - 1}}$... (3)	$\frac{R_a}{R_1} = 0.61 \exp \left(\frac{1 - \beta}{F_c} \right)$... (8)
$\frac{U_{Ra}}{R_1} = \gamma_t \cdot H \left[1 - \frac{F_c}{\zeta - 1} \left\{ \left(\frac{R_a}{R_1} \right)^{\zeta - 1} - 1 \right\} - \beta \left(\frac{R_a}{R_1} \right)^{\zeta - 1} \right] \cdot \frac{1 + \nu}{E_{cu}} \left(\frac{R_a}{R_1} \right)$... (4)	$\frac{U_{Ra}}{R_1} = \gamma_t \cdot H \left(1 - \beta - F_c \ln \frac{R_a}{R_1} \right) \cdot \frac{1 + \nu}{E_{cu}} \left(\frac{R_a}{R_1} \right)$... (9)
$p' = (\sigma'_r + \sigma'_\theta) / 2$... (5)	$p = (\sigma_r + \sigma_\theta) / 2$... (10)
$\frac{U_a}{R_1} = 1 - \sqrt{1 - \left(\frac{R_a}{R_1} \right)^2 + \left(\frac{R_a}{R_1} - \frac{U_{Ra}}{R_1} \right)^2}$... (11)	

Note: $\zeta = (1 + \sin \phi) / (1 - \sin \phi)$, E_{cu} : Young's modulus by CU test, $\beta = \sigma_i / \sigma_o$, $F_c = q_u / \sigma_o$, $\sigma_o = \gamma_t \cdot H$ ν : Poisson's ratio

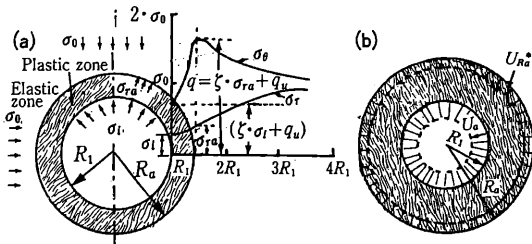


Fig. 5 Stresses around a deep circular tunnel in elastic-plastic state (a) and deformation (b)

overburden of $H = 150\text{m}$ with $\gamma_t = 20\text{kN/m}^3$, where earth pressure and convergence were measured (ref. Fig. 2), $q_u = 13 \times 10^2\text{kPa}$ which corresponds to $w_a = 25\%$. Therefore, for the short-term after excavation $F_c = (13 \times 10^2) / (3 \times 10^3) = 0.43$.

Substituting these values, the relationship between $\beta = \sigma_i / (\gamma_t \cdot H)$ and U_a / R_1 (or $2U_a$) is obtained as a solid line in Fig. 6. For the long-term, $F_c = 0$ and the relationship between β and U_a / R_1 is obtained as a dashed line in Fig. 6. Fig. 2 shows that the earth pressure equilibrated after a short-term is $\sigma_i = 4 \times 10^2\text{kPa}$ i.e. $\beta = 4 \times 10^2 / 3 \times 10^3 = 0.13$. Fig. 2 also shows that the corresponding convergence is 40cm. However, it is generally accepted that, in a squeezing tunnel,

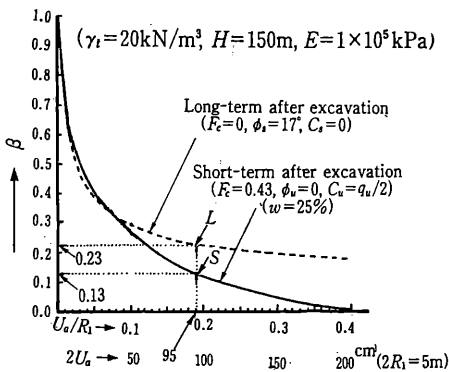


Fig. 6 Relationship between $\beta = \sigma_i / (\gamma_t \cdot H)$ and convergence $2U_a$.

the absolute convergence is approximately twice the value observed after the tunnel face has reached the observation point, thus $2U_a = 80\text{cm}$ or $2U_a / 2R_1 = 0.16$ being suggested in this case. The convergence ratio U_a / R_1 , corresponding to $\beta = 0.13$ is 0.19 or $2U_a = 95\text{cm}$ which is of the same order of magnitude of the value quoted above. The dashed line in Fig. 6 shows that β increases to 0.23 after a long-term if the convergence is restricted at $U_a / R_1 = 0.19$, indicating that earth pressure slowly increases up to $6.9 \times 10^2\text{kPa}$ and it exerts pressure even on an inner lining. The long-term earth pressure has not been reported for this case but recent investigation has revealed that not a few cracks were found in the inner concrete lining of the tunnel, suggesting that the earth pressure increased for the past long time. From the relationships of $q \sim w$, $w \sim p'$ shown in Fig. 3, 4, $F_c = (0.95 \pm 0.15) h^{-0.18}$ can be derived which substantiates the general experience that the deeper the tunnel, the worse the excavation condition in faulted zone is.

Thus, the so-called swelling pressure has been explained successfully using strength parameters only, without recourse to any data on swelling capacity of clay.

5.2 Increase in water content around a tunnel

Substituting $\sigma_i = 6.9 \times 10^2\text{kPa}$ into equations (1), (2) and $\sigma_i = 4.0 \times 10^2\text{kPa}$ into equations (6) (7), p' and p can be calculated by equation (5) (10) whose distributions are shown in Fig. 7.

Although p decreases from the initial stress σ_o in the short-term case, the corresponding effective stress p' is kept constant at the ini-

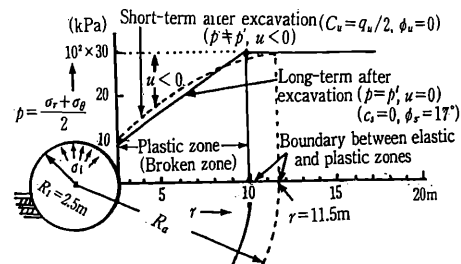


Fig. 7 Distribution of average confining stress

tial stress $p' = p - u = \sigma_0 = 3 \times 10^3 \text{ kPa}$, because of the negative pore pressure $u < 0$. As time elapses, this pore pressure is dissipated and water is sucked into either narrow shear bands (which develop within broken zone) along the fully-softened state line or into unsheared block along the rebound line in Fig.4. As w_s is a function of r' which is a function of r (m), the water content distribution long after excavation can be expressed as a function of r . Fig.8 shows the water content distribution thus calculated together with the distribution of density ρ_t which is a function of w , therefore, of r .

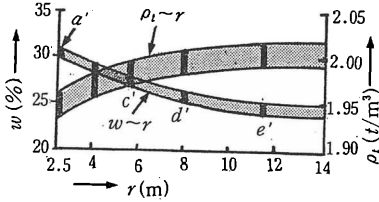


Fig.8 Increase in water content and decrease in wet density in a plastic zone

The actual distributions of w and ρ_t show the similar tendency. These observed data give an apparent impression that the swelling of clay is the main cause of swelling tunnel, but the swelling is the result of the formation of broken zone and not the cause of it. Therefore, it is better to use "Squeezing-swelling rock" instead of "Swelling rock" for incompetent mudstone.

6. PROPOSAL FOR SIMPLE DESIGN PROCEDURE OF A SQUEEZING-SWELLING TUNNEL

Based on the mechanism of squeezing-swelling in tunneling, the flow-chart of a simple design procedure is proposed as shown in Fig.9.

7. CONCLUSION

The real predominant cause of "so-called swelling tunnel" is not the increase in volume of the ground due to swelling of mudstone but just the plastic flow of the plastic (broken) zone around a tunnel, although the water content around a tunnel is increased accompanying the decrease in average effective stress in the plastic zone long after excavation. Therefore, the swelling test of clay specified by "Standard design specification for tunnels" by JSCE for potential swelling tunnels should be discarded.

ACKNOWLEDGEMENT

The authors are grateful to JRCP for access to the construction site of Nabetachiyama Tunnel to take samples and for their providing us the observed data.

REFERENCES

Atkinson J.H., Evans J.S. & HO E.W.L.(1985). Non-uniformity of triaxial sample due to consolidation with radial drainage. *Geotechnique* 35, No.3, 353-355
 Kastner H.(1962). *Statik des Tunnel und Stollenbaues*. Springer-Verlag, Berlin, 101
 Kojima K.(1990). Construction of Nabetachiyama Tunnel. *Dobokugijyutsu* 45, No.8, 68-78
 Nakano R.(1979). Geotechnical properties of mud-

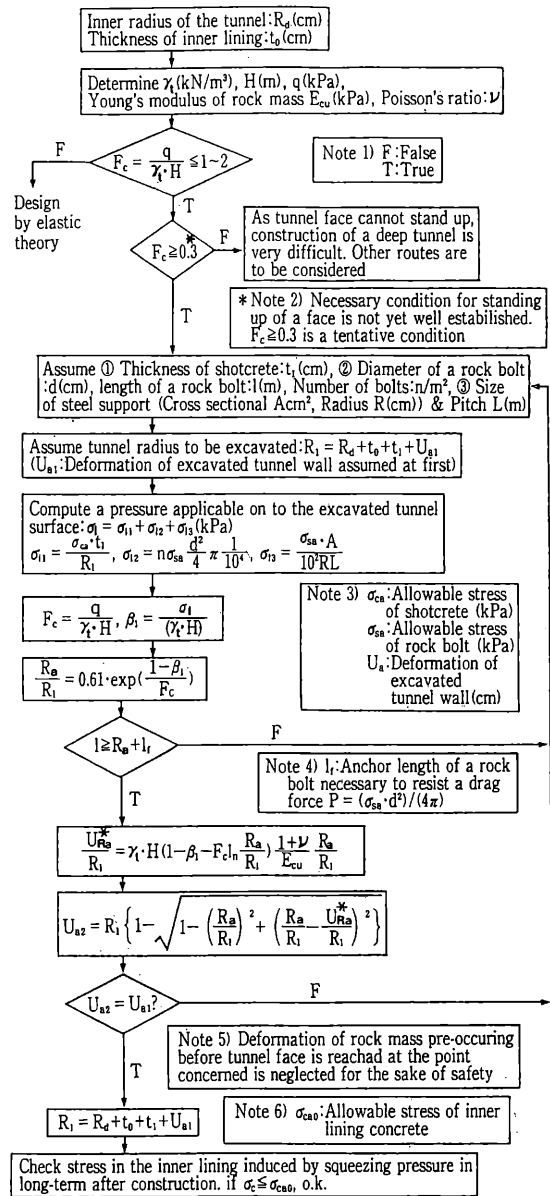


Fig.9 Tentative proposal of a simple design procedure of a deep relatively small circular tunnel ($2R_1 \leq 5m$) driven by full face method through soft mudstone or its fault clay by NATM, assuming $K=1$

stone of Neogene Tertiary in Japan with special reference to the mechanism of squeezing-swelling rock pressure in tunneling, *Proc.Int. Symp. on Soil Mechs.*, Oaxaca, Mexico, 75-92
 Ohtsuka M. & Takano A.(1980). Displacement due to tunnel excavation & geological characteristics in swelling mudstone. *Tsuchi-to-kiso*, No. 270, 29-36
 Skempton A.W. & Sowa V.A.(1963). The behaviour of saturated clays during sampling and testing. *Geotechnique* 13, No.4, 269-290
 Terzaghi K.(1964). Rock tunneling with steel supports, *The Commercial Shearing & Stamping Co.*, Youngstown, Ohio, 81-83